F^{19}, Na^{23}, and $Al^{27}(\alpha,n)$ Reactions*

R. M. WILLIAMSON, T. KATMAN, AND B. S. BURTON†
Duke University, Durham, North Carolina

(Received September 28, 1959)

The F^{19}, Na^{23}, and $Al^{27}(\alpha,n)$ yield curves are given from threshold to about 4 Mev. Convenient resonances for alpha particle energy calibration in these reactions and in the $C^{13}(\alpha,n)$ reaction are pointed out. "Slow-fast" neutron data and γ ray data for $F^{19}(\alpha,n)$ agree with the proposed 593- and 666-kev Na^{22} levels. The Al^{26m}(228 kev) β activity was observed in the $Na^{23}(\alpha,n)$ reaction. The neutron resonance absorption technique gave $Q=-1959\pm10$ kev for $F^{19}(\alpha,n)$. The $32°\pm3°$ angle cut-off of $Na^{23}(\alpha,n)$ neutrons at $T_\alpha=3492\pm3$ kev gave a Q value of -2969 ± 4 kev. The threshold for P^{30} β activity gave $Q\geqslant-2662\pm5$ kev for $Al^{27}(\alpha,n)$.

THERE is currently considerable uncertainty in the atomic masses between oxygen and sulphur.[1] (α,n) reaction Q values have the advantage of linking nuclei which differ by two charge units and three mass units, but they have the disadvantage of being difficult to measure. We chose to study the F^{19}, Na^{23}, and $Al^{27}(\alpha,n)$ reactions because they have negative Q values,[2] and one could, in principle, measure accurate threshold energies for them. Further, no detailed yield curves exist[2] for these reactions, and the product odd-odd self mirror nuclei are interesting.[3,4] Also, we hoped that these thresholds would provide convenient alpha particle calibration points for accelerator beam magnetic analyzers. We report the $C^{13}(\alpha,n)$ reaction here because it appeared as an unavoidable contamination, and because it provided a useful energy calibration point.

Singly ionized alphas were available from a 4-Mev electrostatic accelerator. A one meter radius cylindrical electrostatic analyzer[5] defined both the incident beam energy and the energy spread. By observing the 992-kev $Al^{27}(p,\gamma)$ resonance and the $Li^7(p,n)$ threshold with both the H^+ and the HH^+ beams, we found the analyzer linearity to be better than 1/1000 in energy between about 1 and 4 Mev. We have assumed a comparison uncertainty of 1/2000 for the energy intervals involved in the following data. The value 1.8811 Mev was used as the energy of the $Li^7(p,n)$ threshold.[6]

Targets of LiF, CaF_2, NaCl, and Al were evaporated onto 10 mil tantalum end caps. Even though the evaporator had a liquid air trap, background $C^{13}(\alpha,n)$ neutrons from the natural carbon contamination of these targets proved to be a problem. Somewhat cleaner fluorine targets were made by warming hydrofluoric acid on the tantalum end caps and then rinsing them with water. These targets were not completely stable nor did they have a uniform density. Carbon build-up is, of course, a much more serious source of incident beam energy uncertainty for alphas than for protons of moderate energy. We found that a liquid air cooled charcoal trap located a few inches from the target kept the carbon build-up less than several kev per hour of running with a 5 μa beam. Fresh target spots were used to check the rate of carbon build-up.

Total cross-section data (Table I, Figs. 6 and 9) were taken with a shielded, paraffin-BF_3 counter matrix in the form of a hollow cylinder.[7] The axis of the cylinder was parallel to the beam tube, and the target was at the center of the cylinder. Neutrons emitted in the forward direction were scattered into the matrix by a carbon block. Our McKibben matrix[8] was modified so as to contain a 1-in. diameter counter filled with 100 cm of enriched BF_3. We have found that this counter has a flat neutron response and a counting efficiency of 1.25%. We made no special efforts to determine absolute cross sections; the numbers quoted here are uncertain to about $\pm30\%$. However, we believe that counting conditions and estimated cross sections should be published with all yield curves. The "slow-fast" neutron counters were similar to Bonner's.[9] The axis of the "slow" counter and the front face of the "fast" counter were 1.5 and 3 in. from the target spot, respectively. The neutron data in Figs. 4 and 7 were taken with a 1-in. diameter, 100 cm, enriched BF_3 counter surrounded by a $\frac{3}{4}$ in. thick, 8 in. long paraffin sleeve; the counter was perpendicular to the beam tube. Beta activities were detected with a thin end-window Geiger counter.

Three of the four $C^{13}(\alpha,n)$ resonances already reported[10,11] at 2.60, 2.67, 2.76, and 2.80 Mev are seen as part of the background in Figs. 2 and 9. The "slow-fast" neutron counter ratio (S/F) also serves to identify

* This work was supported by the U. S. Atomic Energy Commission.

† Present address: Convair, Fort Worth, Texas.

[1] H. Hintenbergen, *Nuclear Masses and their Determination* (Pergamon Press, New York, 1957).

[2] P. M. Endt and C. M. Braams, Revs. Modern Phys. **29**, 683 (1957).

[3] P. Stähli, Phys. Rev. **92**, 1076 (1953).

[4] S. A. Moskowski and D. C. Peaslee, Phys. Rev. **93**, 455 (1954).

[5] Warren, Powell, and Herb, Rev. Sci. Instr. **18**, 559 (1947).

[6] Jones, Douglas, McEllistrem, and Richards, Phys. Rev. **94**, 947 (1954).

[7] Block, Haeberli, and Newson, Phys. Rev. **109**, 1620 (1958).

[8] A. O. Hansen and J. L. McKibben, Phys. Rev. **72**, 673 (1947).

[9] Brugger, Bonner, and Marion, Phys. Rev. **100**, 84 (1955).

[10] Bonner, Kraus, Marion, and Schiffer, Phys. Rev. **102**, 1348 (1956).

[11] Walton, Clement, and Boreli, Phys. Rev. **107**, 1065 (1957).

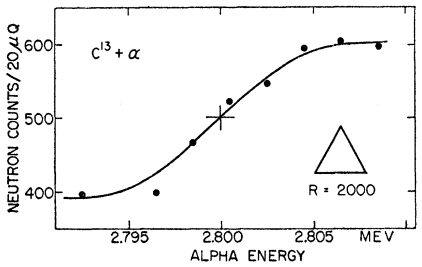

FIG. 1. (α,n) yield from a semithick natural carbon target taken with a McKibben counter at 0° and 3 in. from the target.

the fast neutrons from $C^{13}(\alpha,n)$ in Fig. 2. We took data on natural carbon to aid in estimating the background in our reaction data. A careful study of the highest of the four $C^{13}(\alpha,n)$ resonances is seen in Fig. 1; this resonance at 2800±3 kev has a width of about 4 kev. The previously reported energies and widths for this resonance are 2805±5(11)[11] kev and 2825($\leqslant$7) kev.[10]

Figures 2 and 3 show that the first strong $F^{19}(\alpha,n)$ resonances are spaced about 100 kev apart and are less than 20 kev wide. There is very little yield between resonances, and the peak cross sections are low. (See Table I.) We made a careful study with semithick targets of the positions and shapes of resonances A, B, and C. These three energies in Table I are accurate to ±3 kev; the widths are 8, 11, and 6 kev, respectively. (Figure 4 shows data at resonance C.) The other resonance energies are uncertain by about 10 kev because the target thickness was comparable to the resonance widths. Figure 3 also shows a $F^{19}(\alpha,p'\gamma)$ resonance at 2738±3 kev with a width of 9 kev which is quite separate from the nearby $F^{19}(\alpha,n)$ resonance C. We found that $F^{19}(\alpha,n)$ resonances A through D did not coincide with similarly spaced $(\alpha,p'\gamma)$ observed at 2.46, 2.53, 2.63, 2.738, and 2.81 Mev. Sherr, Li, and Christy[2] have reported $F^{19}(\alpha,p'\gamma)$ resonances at 2.463, 2.533, 2.648, and 2.758 Mev.

The S/F ratio in Fig. 2 leads to an estimate of 2.36 Mev for the $F^{19}(\alpha,n)$ reaction threshold. A very careful and unsuccessful search for this threshold was made with a rinsed hydrofluoric acid target and the total cross-section counting matrix. The S/F ratio gives no evidence for a Na^{22} excited state lower than 593 kev. The increase in the S/F ratio and the onset of 593-kev gamma rays seen in Fig. 3 at resonance J(3.12 Mev) occurs just above the 3.09 Mev threshold calculated for the $F^{19}(\alpha,n'\gamma)Na^{22*}$ (593 kev). The threshold for the $F^{19}(\alpha,n'\gamma)Na^{22*}$ (666 kev) reaction should be at 3.18 Mev. (We have used our ground state Q value of −1959 kev and the 593- and 666-kev level energies reported by Temmer[12] to calculate these expected thresholds.) The S/F ratio at resonance M(3.30 Mev) is 12% too large to be explained solely by the presence of neutrons

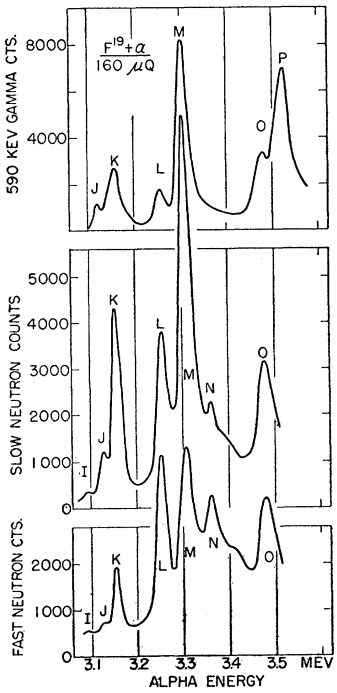

FIG. 3. (α,n) yields continued from Fig. 2 plus the photopeak yield of $(\alpha,n'\gamma)$ 593-kev gammas taken with a 2×2 in. NaI counter at 90° and 5 in. from the target.

to the 593 Na^{22} excited state, and therefore a Na^{22} level at an energy between 600 and 760 kev is indicated by our data. The uncertainty in our S/F ratio at resonance M, due to the difficulty in assigning the background underneath the resonance, is about 8%, and thus our evidence for the 666-kev level is not strong. We were unable to detect 73-kev cascade gammas at resonance M in the presence of other low-energy gammas.

By use of an O^{16} absorber it is possible to detect the presence of 433-kev neutrons because of a strong, isolated oxygen resonance at that energy.[13] Since the $F^{19}(\alpha,n)$ reaction has only isolated, narrow resonances, one can achieve continuous neutron energy variation

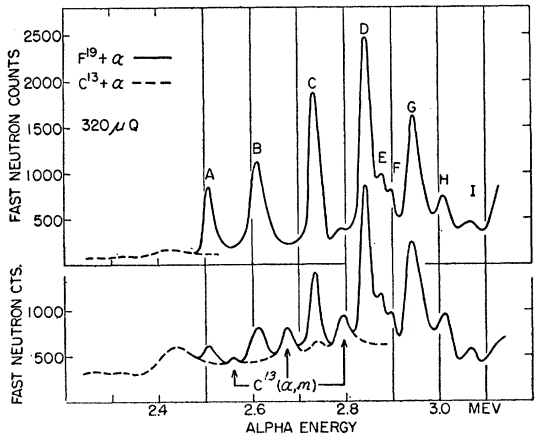

FIG. 2. (α,n) yields from a CaF_2 target taken with Bonner-type counters. The data points were spaced 10 kev, and the target was about 20 kev thick.

[12] G. M. Temmer and N. P. Heydenburg, Phys. Rev. **111**, 1303 (1958).

[13] F. Ajzenberg-Selove and T. Lauritsen, Nuclear Phys. **11**, 1 (1959).

through the 433-kev oxygen resonance by changing the sample and counter angle relative to the alpha beam. The S/F data of Fig. 2 indicated that 433-kev neutrons should be emitted at a convenient forward angle of about 25° in the laboratory system at resonance *C* (2730 kev). Further data showed resonance *C* to be isotropic in the c.m.system. In order to analyze the oxygen transmission as a function of neutron angle data (Fig. 5), we took similar data using $Li^7(p,n)$ neutrons at proton energies chosen so as to give 433-kev neutrons near 25°. The neutron yield and energy changes with angle are roughly the same for the $F^{19}(\alpha,n)$ and $Li^7(p,n)$ reactions at the incident energies used here.

The data of Fig. 5 were taken with a McKibben counter 20 in. from the target and a BeO disk ($3\frac{3}{4}$-in. diameter, $3\frac{1}{4}$ in. thick, 70.4 g/cm³ density) placed between the target and the counter so that it subtended the same angle as the counter. The effective counter acceptance angle was ±9°. The low counting rates required relatively poor geometry and imposed the major limitation on resolving the oxygen resonance. The angular distribution of the transmission through

TABLE I. Energies and total cross sections of neutron resonances shown in Figs. 2 and 3.

	Mev	mb		Mev	mb
A	2.498	3	*I*	3.07	7
B	2.609	6	*J*	3.12	3.5
C	2.730	14	*K*	3.15	25
D	2.84	16	*L*	3.25	20
E	2.87	2	*M*	3.30	25
F	2.90	2	*N*	3.36	25
G	2.94	10	*O*	3.47	17
H	3.01	3.5			

our BeO sample was taken by use of a 15 kev LiF target. However, the effective alpha energy spread was 8 kev, the natural width of the resonance combined with the beam energy spread. At each neutron angle the BeO transmission was measured below, on, and above $F^{19}(\alpha,n)$ resonance *C*. The 640 μ coul. run at each energy took 3 minutes. Each set of runs was repeated several times in order to keep track of the condition of the target. The counts below and above the resonance were averaged to determine the background beneath resonance *C*. The $Li^7(p,n)$ data were taken with a 5 kev thick LiF target.

A comparison of the $F^{19}(\alpha,n)$ and $Li^7(p,n)$ data taken at 20°, 40°, and 50° (Fig. 5) shows that our ability to get the correct magnitude of (1/Transmission) on (20°) and off (40° and 50°) the 433-kev oxygen resonance is reasonably indicated by the statistical errors. The 0°, 10°, 30° points favor the solid curve and give some bias toward the dotted curve. We conclude that the $Li^7(p,n)$ data taken so as to give 433-kev neutrons at 26° gives the best fit. The estimated ±5° uncertainty in the comparison of the $F^{19}(\alpha,n)$ and $Li^7(p,n)$ data is ±8 kev in the $F^{19}(\alpha,n)$ *Q* value; the errors in incident beam energy, the O^{16} resonance energy, and the current

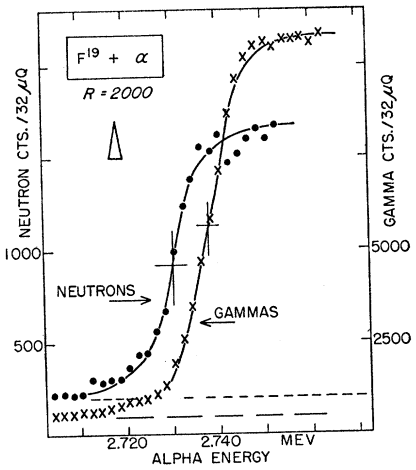

FIG. 4. $F(\alpha,n)$ and $(\alpha,p'\gamma)$ 1.28-Mev gamma yield from a semithick CaF_2 target. The slow neutron counter was at 0° and 2 in. from the target and the 2×2-in. NaI gamma counter was at 90° and 5 in. from the target.

integration combine so as to make the total rms error in the *Q* value ±10 kev. The calculated $F^{19}(\alpha,n)$ *Q* value is −1959±10 kev.

The $Na^{23}(\alpha,n)Al^{26}$ yield curve (Fig. 6) shows levels spaced about 40 kev apart having widths comparable to, or less than, the incident beam energy spread of 4 kev. Again, there is little yield between resonances. The energies of resonances *B* through *G* are: 3536, 3583, 3607, 3655, 3787, and 3832 kev. These are accurate to ±5 kev. More thorough data (Fig. 7) showed resonance *A* at 3492±3 kev to have a natural width <1 kev and a total cross section of 5 mb if a 1-kev level width is assumed. Other data[2] attributes the 6.6 sec positron activity of Al^{26} to a metastable 0^+ level at 228 kev. We have observed beta activity having this half-life beginning at 3.83-Mev alpha energy in qualitative agreement with the proposed Al^{26} level scheme.

Since $Na^{23}(\alpha,n)$ resonance *A* is very close to the expected threshold, we were able to measure to maximum angular opening in the laboratory system of the forward cone of neutrons at this resonance. Since resonance *A* is very narrow, we were able to use a thick

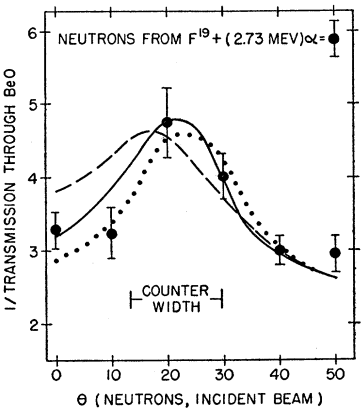

FIG. 5. The dashed, solid, and dotted 1/Transmission vs θ curves were taken using the $Li^7(p,n)$ reaction and proton energies of 2.195, 2.202, and 2.209 Mev, respectively; neutrons of 0.433-Mev energy were emitted at 21.5°, 25.0°, and 27.5°, respectively. The data points were taken with $F^{19}(\alpha,n)$ neutrons, and the errors are statistical.

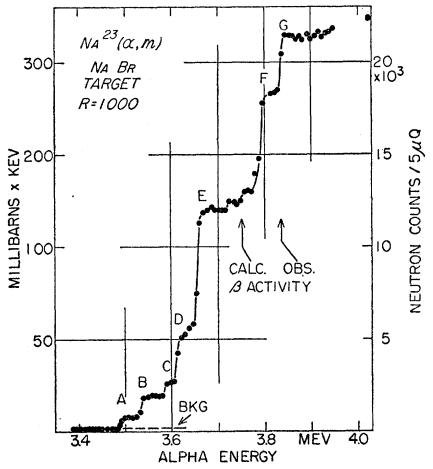

FIG. 6. Total (α,n) yield from a thick NaBr target. The calculated and observed thresholds for beta activity from the 228-kev isomeric state in Al^{26} are shown.

target and take neutron angular distributions at energies just below and just above the resonance. (See Fig. 8.) Obviously we did not have to worry about carbon build-up or other possible beam energy shifts during the runs. In order to fit these data, we assumed an isotropic neutron yield in the center-of-mass system. The cross section in the laboratory system peaks sharply, even after one includes the effect of the large acceptance angle of the neutron counter. (Solid curve Fig. 8.) The angle cutoff is $32°\pm3°$. Using $T_\alpha=3492\pm3$ kev, one gets a $Na^{23}(\alpha,n)$ Q value of -2969 ± 4 kev.

Figure 9 shows $Al^{27}(\alpha,n)P^{30}$ total cross-section data. Again, $C^{13}(\alpha,n)$ background obscures the neutron yield below resonance A. The size of the 2800-kev carbon resonance allowed us to make a good estimate of the background. The Al neutron yield was too low to allow the taking of reasonable neutron resonance absorption data or S/F counter data. However, the 3.5 sec beta activity[2] of P^{30} was first observed at 3056 ± 5 kev; this makes the reaction $Q\geqq-2662\pm5$ kev. Resonances A through G shown in Fig. 8 have the following energies: 3.42, 3.58, 3.68, 3.72, 3.76, 3.81, 3.90 Mev. Only the energy of the first resonance is given for the multiple levels.

The small cross sections observed for these three

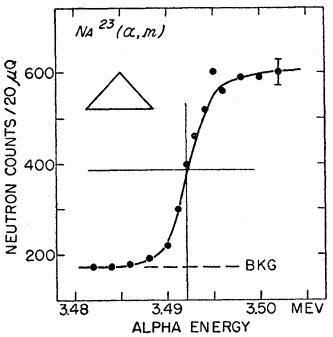

FIG. 7. (α,n) yield from a thick NaBr target. The slow neutron counter was at 0° and 2 in. from the target.

(α,n) reactions are not surprising in view of the possible alpha and neutron orbital angular momenta required. Assuming the nuclear spins and parities given in reference 2, (L_α, L_n) must be (2,0), (1,1), or (0,2) for the F^{19} and $Al^{27}(\alpha,n)$ reactions, while $Na^{23}(\alpha,n)$ requires (4,0), (3,1), (2,2), etc. It is difficult to make arguments about the expected relative heights of resonances near threshold because one does not know the relative sizes of Γ_α, Γ_n, and Γ. However, if one assumes that nuclear reduced widths do not vary greatly in a limited incident energy region and that Γ_n is the major factor controlling the increasing cross sections near threshold, then the relative strengths of the first four resonances

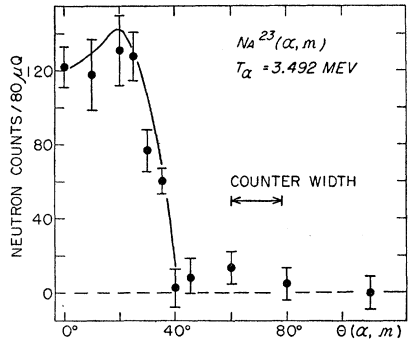

FIG. 8. Angular distribution of neutrons at the 3492-kev $Na^{23}(\alpha,n)$ resonance. A McKibben counter 20 in. from the target was used. The data points are the differences of counts above and below the thick target resonance, and the errors are statistical.

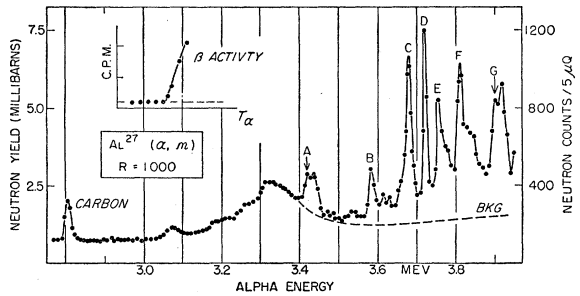

FIG. 9. (α,n) yield from an Al target about 10 kev thick. The inset shows the P^{30} activity of a thick Al target. Assuming a nonresonance $Al^{27}(\alpha,n)$ cross section at 3.1 Mev, the cross section here is about 0.3 μb.

of both the F^{19} and $Na^{23}(\alpha,n)$ reactions follow closely the assumption of $L=0$ neutrons. If one assumes $L=1$ neutrons, the observed ratio of the fourth resonance to the first resonance is a factor of 4 too low in the case of F^{19} and a factor of 100 too low in the case of Na^{23}. The observed isotropy of resonance C in the $F^{19}(\alpha,n)$ reaction very strongly suggests $L_n=0$ for this particular resonance. $(L_\alpha,L_n)=(0,2)$ is very unlikely on penetrability grounds, and $(L_\alpha,L_n)=(1,1)$ gives rise to a uniquely defined angular distribution with an anisotropy of $+33\%$. The fact that the $Al^{27}(\alpha,n)$ reaction shows no observable resonances within 350 kev of its threshold and then has an average level spacing of about 50 kev is interesting.

TABLE II. The mass differences (kev) in the first column employ our (α,n) Q values and the Mg^{24}, Si^{28}, and $S^{32}(d,\alpha)$ Q values of 1953±12,[a] 1428±4,[b] and 4887±11 kev,[c] respectively. The n, d, and α masses given in Wapstra[d] have also been used. The other three mass differences use values given by Wapstra[d] and Nier[e] based on Q values and values by Nier[e] based on mass spectroscopic data. The Δ's are the discrepancies between Wapstra's and Nier's mass differences and those of column one.

	$(\alpha,n)(d,\alpha)$	Wapstra	Δ	Nier (Q)	Δ	Nier (M)	Δ
$Mg^{24}-F^{19}-5$	−10 966±17	−10 995±16	−29	−10 981±21	−15	−10 960±3	+6
$Si^{28}-Na^{23}-5$	−10 482±10	−10 502±21	−20	−10 502±27	−20	−10 494±8	−12
$S^{32}-Al^{27}-5$	−7329±14	−7343±30	−14	−7343±36	−14	−7320±3	+9

[a] See reference 14.
[b] C. P. Brown, Phys. Rev. **114**, 807 (1959).
[c] See reference 2.
[d] See reference 15.
[e] See reference 16.

There is quite likely an absence of $L_n=0$ levels in this region above threshold.

While the F^{19}, Na^{23}, and $Al^{27}(\alpha,n)$ reactions do not have observable neutron thresholds, they have fairly narrow, well separated resonances which could be useful as alpha energy calibration points. Since the yields are small, beam currents of several microamperes are necessary. A LiF target would be quite convenient for the Li+p, Li+α, and F+α reactions. Suggested alpha-energy calibration points are: $Li^7(\alpha,\gamma)$ 0.958 Mev[13]; $F^{19}(\alpha,p'\gamma)$ 1.88 Mev[2]; $F^{19}(\alpha,n)$ 2.730 Mev; $F^{19}(\alpha,p'\gamma)$ 2.738 Mev; $C^{13}(\alpha,n)$ 2.800 Mev; $Na^{23}(\alpha,n)$ 3.492 Mev. All of these resonances but the one in $Na^{23}(\alpha,n)$ are 5 to 10 kev wide, and it is therefore not possible to locate them more accurately than several kev. We believe that semithick targets are usually the most convenient for the study of resonance positions and widths.

The $F^{19}(\alpha,n)$ may be used in two reaction cycles in order to check the observed Q value.

(1)	$+F^{19}(\alpha,p)Ne^{22}$	+1673±11 kev[14]
	$-Na^{22}(\beta)Ne^{22}$	−2840± 9 kev[2]
	$-F^{19}(\alpha,n)Na^{22}$	+1959±10 kev
	$-(n-H)$	− 783± 1 kev[15]
		9±18 kev
(2)	$+Ne^{21}(d,p)Ne^{22}$	+8137±11 kev[14]
	$-Ne^{21}(d,\alpha)F^{19}$	−6432±10 kev[14]
	$-Na^{22}(\beta)Ne^{22}$	−2840± 9 kev[2]
	$-F^{19}(\alpha,n)Na^{22}$	+1959±10 kev
	$-(n-H)$	− 783± 1 kev[15]
		+ 41±20 kev.

[14] D. M. VanPatter and Ward Whaling, Revs. Modern Phys. **29**, 757 (1957) and **26**, 402 (1954).
[15] A. H. Wapstra, Physica **21**, 367 (1954).

The results of these cycles suggest that either the $Ne^{21}(d,\alpha)$ or the $Ne^{21}(d,p)$ reaction Q values are in error, in agreement with the findings of Nier.[16]

The $Na^{23}(\alpha,n)$ reaction Q value may be used in the following reaction cycle.

$+Mg^{25}(d,p)Mg^{26}$	+8880±12 kev[14]
$+Mg^{26}(p,n)Al^{26}$	−4778±15 kev[14]
$-Na^{23}(\alpha,n)Al^{26}$	+2969± 4 kev
$-Mg^{25}(d,\alpha)Na^{23}$	−7019±13 kev[14]
	+ 52±24 kev

Since we believe that the error in our $Na^{23}(\alpha,n)$ Q value is realistic, there appears to be an error in one, or several, of the other three reactions. The $Mg^{26}(p,n)$ Q value agrees within 9 kev of the Al^{26m}(228 kev)$(\beta)Mg^{26}$ Q value of 3.21±0.03 Mev,[2] but this could be fortuitous. An accurate measurement of the $Na^{23}(\alpha,p)$-Mg^{26} Q value would be a most helpful check for this reaction cycle.

No practical closed cycles involving the $Al^{27}(\alpha,n)$ reaction can be made. Measurements of the $P^{30}(\beta)Si^{30}$, $Si^{30}(p,n)P^{30}$, and $Al^{27}(\alpha,p)Si^{30}$ Q values would be valuable.

Table II compares mass differences calculated using (α,n) and (d,α) Q values with mass differences calculated using the mass values of Wapstra[15] and Nier.[16] In general, the (α,n), (d,α) mass differences seem to agree best with those calculations from Nier's spectrographic masses. Table II also shows the value of reaction energies involving alpha particles, i.e., that a mass difference of five may be checked using only two Q values once the light particle masses are well established.

[16] Scolman, Quisenberry, and Nier, Phys. Rev. **102**, 1076 (1956).